nature climate change

LETTERS

PUBLISHED ONLINE: 12 OCTOBER 2014 | DOI: 10.1038/NCLIMATE2397

Time of emergence for regional sea-level change

Kewei Lyu[1,2], Xuebin Zhang[1]*, John A. Church[1], Aimée B. A. Slangen[1] and Jianyu Hu[2]

Determining the time when the climate change signal from increasing greenhouse gases exceeds and thus emerges from natural climate variability (referred to as the time of emergence, ToE) is an important climate change issue[1]. Previous ToE studies were mainly focused on atmospheric variables[2–7]. Here, based on three regional sea-level projection products available to 2100, which have increasing complexity in terms of included processes, we estimate the ToE for sea-level changes relative to the reference period 1986–2005. The dynamic sea level derived from ocean density and circulation changes alone leads to emergence over only limited regions. By adding the global-ocean thermal expansion effect, 50% of the ocean area will show emergence with rising sea level by the early-to-middle 2040s. Including additional contributions from land ice mass loss, land water storage change and glacial isostatic adjustment generally enhances the signal of regional sea-level rise (except in some regions with decreasing total sea levels), which leads to emergence over more than 50% of the ocean area by 2020. The ToE for total sea level is substantially earlier than that for surface air temperature and exhibits little dependence on the emission scenarios, which means that our society will face detectable sea-level change and its potential impacts earlier than surface air warming.

Global mean sea level has been rising[8,9] and is projected to rise further in the future, as indicated by state-of-the-art global climate models[10]. Sea-level changes are not expected to be spatially uniform—that is, one region may experience a very different sea-level change from other regions[11,12]. It is the local relative sea-level changes (in both long-term mean and extreme event statistics) that the local communities directly experience and thus care more about than the global mean[13,14]. However, it is usually difficult to detect sea-level change signals at local scales because of the considerable natural variability[15,16]. The ToE estimated for regional sea level can help us to identify when and where the sea-level change becomes locally evident beyond the natural variability, thus providing useful guidance for local risk assessment, mitigation and adaptation planning associated with sea-level change.

In this study, we examine the ToE of regional sea level with outputs from 17 Coupled Model Intercomparision Project Phase 5 (CMIP5) climate models[17] and recently published regional sea-level projections[18], similar to (but not identical to) the IPCC Fifth Assessment Report projections[10]. Three regional sea-level projection products are used here: I. Regional dynamic sea level (DSL) from dynamical adjustment of the ocean to the changing momentum, heat and freshwater fluxes into the ocean only; II. DSL plus global mean thermosteric sea level (GMTSL), one of the major contributions to global mean sea-level change induced by thermal expansion of sea water[19]; III. Total sea level, comprising DSL, GMTSL and regional sea-level contributions from the contemporary loss of land ice and changes in land water storage, including the associated changes in the Earth's gravitational field and vertical land motion (that is, fingerprints[20]), and a regional contribution as a result of glacial isostatic adjustment (GIA). These three products are used to check whether (and how) various sea-level contributions alter the ToE. Two future Representative Concentration Pathway (RCP) scenarios[21] are analysed: the medium scenario RCP4.5 and the high scenario RCP8.5 among CMIP5 simulations, with global mean sea-level rise relative to 1986–2005 reaching 0.53 and 0.74 m by 2100, respectively[10].

When estimating the ToE, we compare the climate change signal with natural climate variability simulated by the climate models. Specifically, the ToE is defined as the time when the ratio of the climate change signal (S) to the noise of natural variability (N) exceeds a particular threshold and never falls below this threshold again (see two examples in Supplementary Fig. 1). We also add one more criterion that any emergence has to last for a minimum period, as ToEs near the end of projections may not represent the true emergence of change signals[2,22]. Here we choose two decades as the minimum emergence period (see Supplementary Information and Supplementary Fig. 2). The annual regional sea-level projections over 2006–2100 relative to the reference period 1986–2005 are used to quantify S. According to our definition, the latest ToE for our study period 2006–2100 is 2080. The noise N is estimated as the standard deviation of annual DSL over 200 years from the linearly de-trended pre-industrial control experiment, with constant pre-industrial forcing (Supplementary Fig. 3). In this study, the S/N ratio threshold is set to two, thus we aim to detect emergence at 95% confidence level. The ToE is first estimated for each individual model and then the multimodel ensemble (MME) median and 16–84% range are derived (Supplementary Information and Supplementary Fig. 4).

Sea level can vary on various spatial and temporal scales. The natural variability of annual sea level is mainly about year-to-year variations of sea level, induced by internal processes within the climate system (for example, modes of climate variability such as the El Niño Southern Oscillation, meandering of ocean current, varying strength and shifting location of gyre circulation), or variations in natural climate forcing (for example, volcanic eruption and solar activity). The natural variability patterns from the CMIP5 pre-industrial control runs share a number of common features with those derived from the de-trended satellite altimeter observations since 1993 (Fig. 1), although the underlying processes may not be exactly the same. For example, both models and observations show high variability in the tropical Pacific. There are peaks off the equator in the west and on the equator in the east, which are signatures of equatorial wave dynamics. The CMIP5 MME mean shows a weaker variability in the central and eastern equatorial Pacific compared with the altimeter observations. Strong natural variability of sea level occurs in regions with strong currents, including the Kuroshio Extension in the Northwest Pacific, the North Atlantic Current

[1]Centre for Australian Weather and Climate Research; CSIRO Oceans and Atmosphere Flagship, Hobart, Tasmania 7001, Australia, [2]State Key Laboratory of Marine Environmental Science, College of Ocean and Earth Sciences, Xiamen University, Xiamen, Fujian 361102, China. *e-mail: Xuebin.Zhang@csiro.au

© 2014 Macmillan Publishers Limited. All rights reserved.

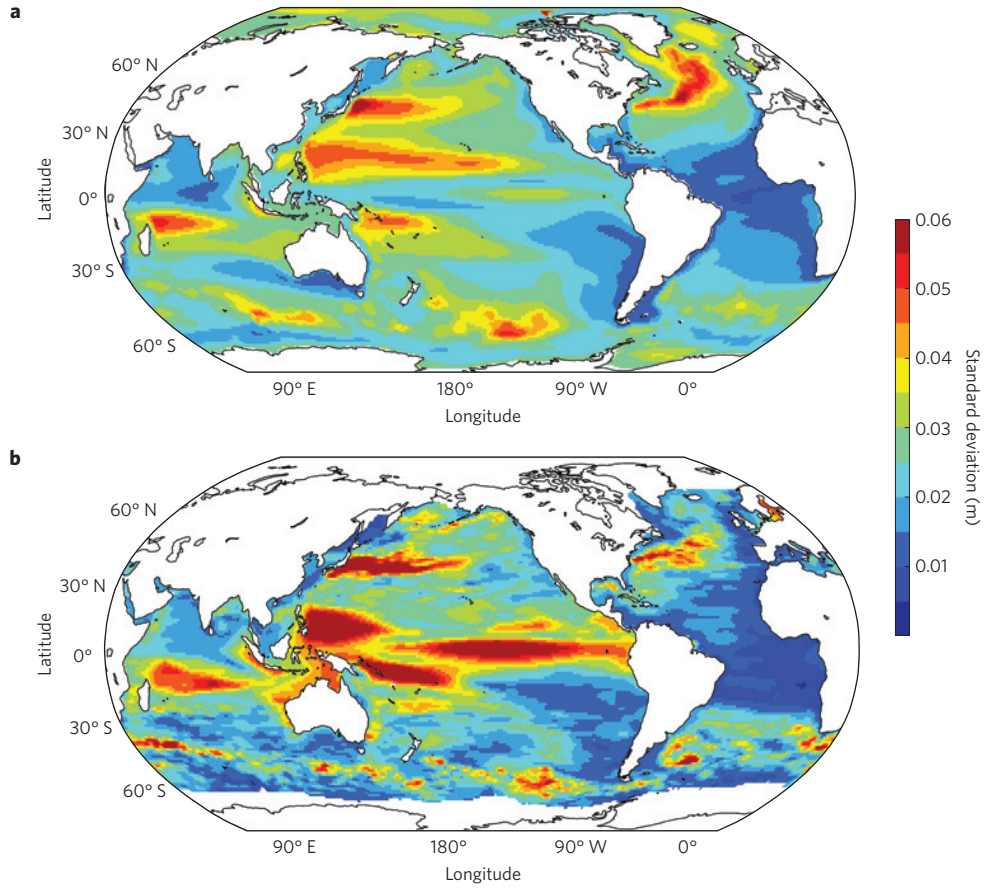

Figure 1 | Standard deviation of annual sea level. a, For CMIP5 multimodel ensemble mean, using de-trended annual dynamic sea-level data from 200-year pre-industrial control runs. **b**, For observations, using de-trended annual sea-level data from 19-year altimeter observations. Note that the detrending of 19-year altimeter observations may also remove some portion of natural sea-level variability at decadal and longer timescales, thus the natural sea-level variability could be slightly underestimated in **b**.

and the Antarctic Circumpolar Current. Regions with weak sea-level variability, including the northern Indian Ocean, the Southeast Pacific and the tropical Atlantic Ocean, are also presented in both altimeter observations and CMIP5 model simulations.

The DSL change signals (product I) emerge from the range of natural variability (that is, twice the standard deviation of DSL from control runs) over only a small fraction of the ocean by 2080 under both scenarios (Fig. 2a and Supplementary Fig. 5). A ToE tends to occur where the local DSL exhibits strong changes, either rising or falling. The overall patterns of ToE show some resemblance to those of DSL projections[11]. Early ToEs with rising signals are found in the Northwest Atlantic, implying that ocean dynamics make a large contribution to sea-level rise in this area[23]. In the Southern Ocean (south of ~50° S), early ToEs with the opposite sign occur owing to a strong DSL fall there. By 2080, the cumulative fraction of the ocean area with emergence increases from 8.8% under RCP4.5 to 18.4% under RCP8.5 based on the MME median ToE (Fig. 3 and refer to Supplementary Fig. 6 for information with other MME percentiles).

When GMTSL is also included in addition to DSL (product II), by 2080 the majority of ocean (92.1% under RCP4.5 and 95.0% under RCP8.5 based on MME median) shows ToEs with rising sea level (Fig. 2b and Supplementary Fig. 5). Regions with earlier ToEs generally correspond to the rising DSL or the weak natural variability, whereas later ToEs are commonly related to the falling DSL or the strong local natural variability. In the Southern Ocean, the cancellation of rising GMTSL and lowering DSL leads to large areas with no emergence before 2080. In some isolated regions of the Southern Ocean, models differ as to what extent regional DSL fall counteracts the GMTSL rise, leading to no agreement on the direction of ToE.

When all other sea-level contributions (loss of land ice, GIA and groundwater depletion) are included (product III), the total sea-level change signals relative to the reference period 1986–2005 emerge over virtually all of the ocean before 2080 (Fig. 3). The ocean area where total sea-level changes emerge against the natural variability rapidly increases before 2030 at a nearly linear rate of about 4% per year for both scenarios. Most of the ocean exhibits rising sea level by 2080, with later ToEs being generally in regions with stronger natural variability. In the MME median patterns, the spatial 50% percentile over the areas with ToEs is 2019 (2011–2028 for 16–84% range) under RCP4.5 (Supplementary Fig. 5) and 2017 (2010–2024) under RCP8.5 (Fig. 2c). Similar values can be obtained when using only grid points along the coastlines. Thus, it takes roughly two to three decades (from the middle of the reference period 1986–2005) for the total sea level to emerge beyond the natural sea-level variability, much faster than the first and second cases with DSL alone and DSL plus GMTSL being considered, respectively. Among the three processes, the loss of land ice is found to be the dominant term to affect ToEs, whereas the GIA is important for certain areas, for example, around the North American continent (see Supplementary Fig. 7 for results excluding the GIA contribution). Besides the DSL contribution mentioned above, the early emergence along the US East Coast also includes a significant contribution from land subsidence due to GIA. There are regions with falling sea levels, resulting from ice mass loss of the adjacent land and reduced gravitational attraction between

© 2014 Macmillan Publishers Limited. All rights reserved.

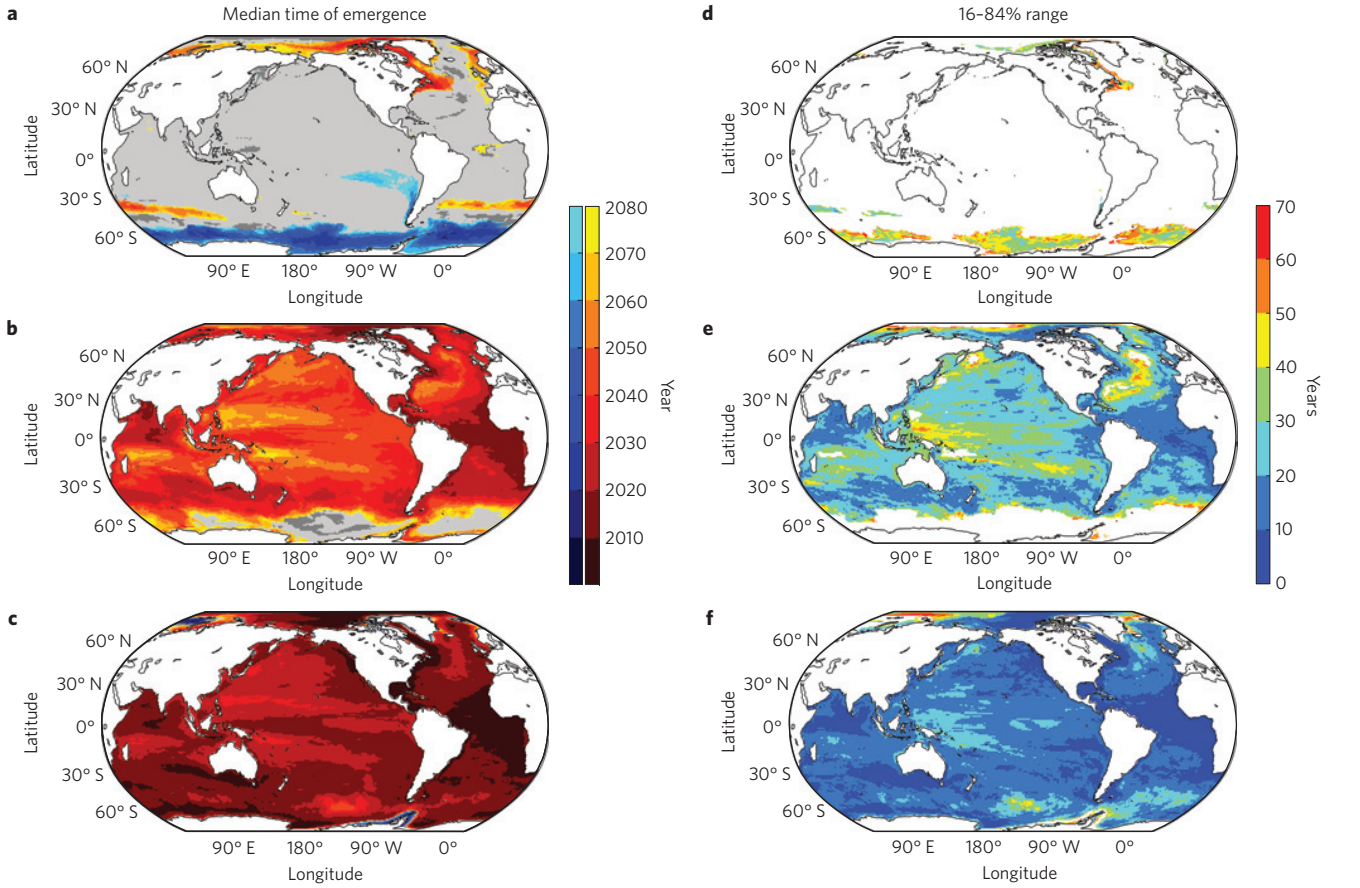

Figure 2 | Multimodel ensemble median ToE for regional sea-level change and the 16–84% range under RCP8.5. Different change signals are used: **a**,**d**, dynamic sea-level change; **b**,**e**, dynamic sea-level change plus global mean thermosteric sea-level change; **c**,**f**, total sea-level change. In the left panels, warm (cold) colours represent rising (falling) sea level; light grey areas have no emergence before 2080; deep grey colour means no agreement among models; white colour means no data coverage or over land. In the right panels, the 16–84% range (years) can be given only where at least 84% models show emergence before 2080.

ocean and land[20]. For example, sea level falls around the Antarctic Peninsula[18] owing to both the nearby loss of land ice and GIA. In the Barents Sea (north of Europe), the GIA is responsible for a regional sea-level fall[18].

The ToE estimates show large differences among models (Supplementary Figs 8–10). When more contributions are included in the sea-level change signals, the models show better agreement on the direction of regional sea-level changes and a smaller MME 16–84% range (Fig. 2 and Supplementary Fig. 5). The smaller uncertainties are generally associated with earlier ToEs. For the total sea level (product III), relatively large uncertainties still exist in the polar areas. There are various sources of inter-model spread, some of which may be narrowed with further model development and improvement (for example, by using better model physics and parameterization). However, some inter-model differences cannot be reduced owing to different phases of natural variability among models[22].

To allow comparison with earlier ToE studies which used different definitions and methods[2–7], we also estimate the ToE for using the same methodology and CMIP5 model ensemble as for sea level. The earliest emergence of surface warming occurs in tropical areas due to the relatively small variability there (Supplementary Fig. 11), consistent with previous studies[2–5]. Under RCP8.5, the cumulative area increase of surface air temperature ToE roughly follows that for DSL plus GMTSL (product II), at a nearly linear rate of about 20% per decade before reaching an 80% cumulative fraction. For RCP4.5, the cumulative area increase of surface air temperature ToE is much slower, with a halved linear rate—that is, 10% per decade (Fig. 3). Relative to 1986–2005, the MME median patterns indicate that 50% of total areas show emergence by the early-to-middle 2040s for surface air temperature under RCP8.5 and DSL plus GMTSL under both RCPs, but it takes two more decades for surface air temperature under RCP4.5 to reach a 50% fraction of area (Supplementary Table 2). This contrast is a result of the longer period required for sea-level rise to become dependent on future greenhouse gas emissions[10,24,25]. We compare the MME projections of GMTSL and global mean surface air temperature to illustrate the difference (Fig. 4). Under RCP8.5, neither global mean surface air temperature nor GMTSL shows a slow-down of positive trends by 2100. However, under RCP4.5 with earlier mitigation[21], surface air responds quickly (from around 2030 the warming rate slows, reaching zero by the end of the twenty-first century), whereas the ocean (in particular the deep ocean) with large thermal inertia takes a longer time to respond[24,25] (the rising GMTSL trend peaks around 2070, then decreases slightly).

The cumulative area increase of surface air temperature ToE over land areas only or over ocean areas only closely follows that over combined land and ocean areas, under both RCPs. That is, there is no significant difference for the time of surface warming emergence between land and ocean, because although the surface warming is stronger over the land than over the ocean[26], the natural variability is also stronger over the land ($0.75 \pm 0.05\,^{\circ}C$) than over the ocean ($0.53 \pm 0.05\,^{\circ}C$).

© 2014 Macmillan Publishers Limited. All rights reserved.

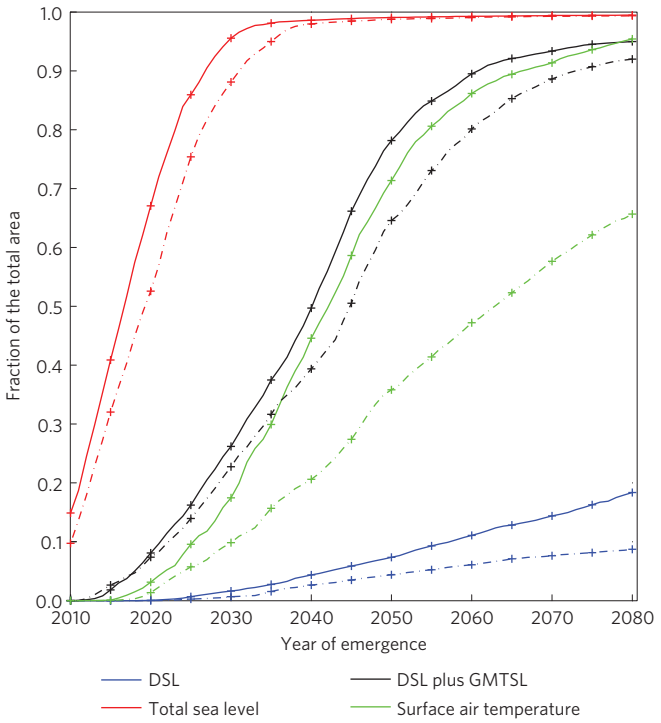

Figure 3 | The cumulative fraction of the total area with the emergence of change signals before the given time from the multimodel ensemble median patterns. Dynamic sea level (blue), dynamic sea level plus global mean thermosteric sea level (black), total sea level (red), surface air temperature (green). Dash-dot lines are for RCP4.5 and solid lines for RCP8.5.

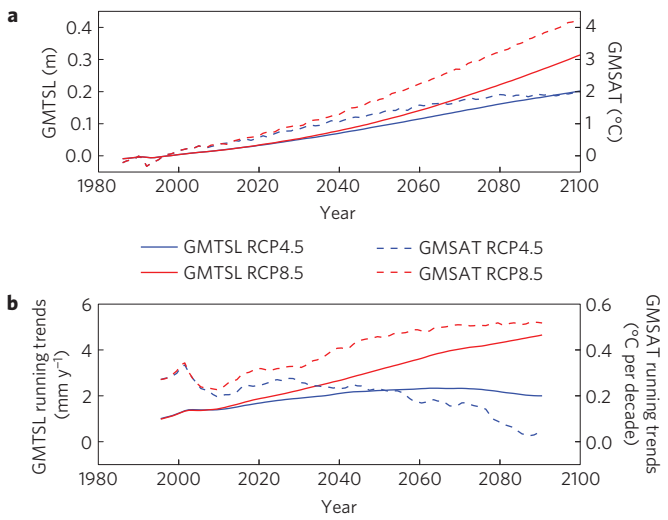

Figure 4 | Multimodel ensemble mean projections of global mean thermosteric sea level (GMTSL) and global mean surface air temperature (GMSAT) under RCP4.5 and RCP8.5. a, Time series of GMTSL and GMSAT over 1986–2100. **b**, 20-year running trends of GMTSL and GMSAT. The left axes are for GMTSL and its running trend (solid lines); the right axes are for GMSAT and its trend (dashed lines).

For both surface air temperature and sea level, the spatial patterns of ToE are largely determined by natural variability—that is, stronger (weaker) natural variability corresponds to later (earlier) ToEs, which means that the improved representation of natural variability in climate models will help to better identify the regional impacts of climate change. The early emergence of rising sea level implies not only the perceptible mean sea-level rise for coastal communities but also an increased likelihood of extreme sea-level events[10]. However, our ability to assess coastal sea-level variability (Supplementary Fig. 12) and change[27] is still limited by the coarse resolution of climate models and non-uniform distribution of *in-situ* observations, which can be addressed by improving observation networks (for example, coastal altimetry) as well as investing in high-resolution modelling.

Methods

Sea-level data and projections. 17 CMIP5 models with all sea-level projection products available are used in our study (Supplementary Table 1). For each model, only the first realization of the available ensemble is used. The sea-level data directly from the model output are the sea surface height above the geoid (labelled as 'ZOS') and global mean thermosteric sea-level change (labelled as 'ZOSTOGA'). The 'ZOS' data for each model grid point and 'ZOSTOGA' data are de-drifted by removing third-order polynomials fitted to the corresponding pre-industrial control runs[28]. The DSL is derived from 'ZOS' by removing its global mean[11]. The inverse barometer correction was not applied because its contribution is relatively small compared with other contributions[10,18]. The land ice and groundwater contributions are adopted from ref. 18. The changes in land ice include mass loss from glaciers and the Greenland and Antarctic ice sheets. Sea-level contributions from both ice sheets were divided into a surface mass balance (SMB) component and an ice dynamics component. The glaciers and SMB contributions were estimated based on CMIP5 model outputs, whereas the ice-sheet dynamics and groundwater contributions were considered to be independent of the climate scenario and model[18]. All the regional sea-level patterns from the land ice and groundwater contributions were computed using a sea-level model which accounts for gravitational, rotational and viscoelastic deformation effects[29]. A more complete description of the methodology and data underlying the land ice and groundwater contributions can be found in ref. 18. Most CMIP5 models do not incorporate freshwater input from ice-sheet loss and thus not all aspects of DSL change have been simulated[10]. The potential collapse of marine-based ice sheets could boost sea-level change signals but reliable estimates are currently unavailable[10]. The regional sea-level change pattern as a result of GIA, which is the delayed response of the earth to land ice loss during the last deglaciation, is from ref. 30. All contributions are applied for all ocean grid points, and re-gridded onto a common $1^\circ \times 1^\circ$ grid. The sea-level data from altimeter observations and models are measured with respect to different reference frames, the centre of the earth and the geoid, respectively. However, the altimeter data are used here only for validation of sea-level variability and thus do not affect our ToE results.

Estimation of natural variability. The natural variability of sea level is estimated here using the linearly de-trended control runs, with the assumption that natural variability derived from control runs remains unchanged in the future. Very similar natural variability patterns are derived when the de-trended time series of various lengths (20, 50 or 100 years) from either historical or RCP runs are used. Natural variability from other contributions should also be considered when the ToE of sea level is not derived from DSL alone (products II & III), but it is found to be negligible in our data. This reflects the dominance of DSL in natural sea-level variability, but could be an artefact of the smoothness of the time series of GMTSL and other contributions, which could be unrealistic. Therefore, our results may slightly underestimate the amplitude of natural variability and, as a result, get earlier ToEs than they should. As a test, if the noise N is increased by 50%, the spatial 50% percentile of the MME median ToE, using total sea level as an example, is delayed by about five years. Following most previous ToE studies[2–6], we focus on sea-level variations on annual and longer timescales by annually averaging all data before analysis. The ToE estimation may be influenced by the timescale over which the original data are averaged, with shorter averaging periods leading to later ToEs (ref. 5).

Sensitivity of ToE estimation to threshold and reference time. For the same level of noise N, a higher threshold means a later ToE and requires stronger signals to reach emergence (Supplementary Fig. 13). However, the ToE spatial patterns are fairly stable, with the threshold ranging from one to three. For the purpose of providing guidance for future climate adaptation, we estimate the ToE with reference to the current-day mean state over 1986–2005. It should be noted that comparison of ToEs from different studies should take reference time differences into consideration. How quickly the climate change signal emerges relative to the reference time depends on the rate of change of the signal (Supplementary Fig. 13). That is, if the rate of sea-level change is constant (that is, linear change with time), the ToE relative to the reference time will be independent of the reference time. However, if the sea-level change accelerates

© 2014 Macmillan Publishers Limited. All rights reserved.

(that is, faster change with time), the ToE will depend on the reference time, for example, quicker (slower) ToE relative to the reference time corresponds to a later (earlier) reference time.

Received 24 June 2014; accepted 4 September 2014; published online 12 October 2014

References

1. Kirtman, B. *et al.* in *Climate Change 2013: The Physical Science Basis* (eds Stocker, T. F. *et al.*) 953–1028 (IPCC, Cambridge Univ. Press, 2013).
2. Diffenbaugh, N. S. & Scherer, M. Observational and model evidence of global emergence of permanent, unprecedented heat in the 20th and 21st centuries. *Climatic Change* **107,** 615–624 (2011).
3. Mahlstein, I., Knutti, R., Solomon, S. & Portmann, R. W. Early onset of significant local warming in low latitude countries. *Environ. Res. Lett.* **6,** 034009 (2011).
4. Hawkins, E. & Sutton, R. Time of emergence of climate signals. *Geophys. Res. Lett.* **39,** L01702 (2012).
5. Mora, C. *et al.* The projected timing of climate departure from recent variability. *Nature* **502,** 183–187 (2013).
6. Mahlstein, I., Portmann, R. W., Daniel, J. S., Solomon, S. & Knutti, R. Perceptible changes in regional precipitation in a future climate. *Geophys. Res. Lett.* **39,** L05701 (2012).
7. Giorgi, F. & Bi, X. Time of emergence (TOE) of GHG-forced precipitation change hot-spots. *Geophys. Res. Lett.* **36,** L06709 (2009).
8. Church, J. A., Monselesan, D., Gregory, J. M. & Marzeion, B. Evaluating the ability of process based models to project sea-level change. *Environ. Res. Lett.* **8,** 014051 (2013).
9. Gregory, J. M. *et al.* Twentieth-century global-mean sea level rise: Is the whole greater than the sum of the parts? *J. Clim.* **26,** 4476–4499 (2013).
10. Church, J. A. *et al.* in *Climate Change 2013: The Physical Science Basis* (eds Stocker, T. F. *et al.*) 1137–1216 (IPCC, Cambridge Univ. Press, 2013).
11. Yin, J. Century to multi-century sea level rise projections from CMIP5 models. *Geophys. Res. Lett.* **39,** L17709 (2012).
12. Zhang, X., Church, J. A., Platten, S. M. & Monselesan, D. Projection of subtropical gyre circulation and associated sea level changes in the Pacific based on CMIP3 climate models. *Clim. Dynam.* **43,** 131–144 (2014).
13. Nicholls, R. J. & Cazenave, A. Sea-level rise and its impact on coastal zones. *Science* **328,** 1517–1520 (2010).
14. Cazenave, A. & Le Cozannet, G. Sea level rise and its coastal impacts. *Earth's Future* **2,** 15–34 (2014).
15. Calafat, F. M. & Chambers, D. P. Quantifying recent acceleration in sea level unrelated to internal climate variability. *Geophys. Res. Lett.* **40,** 3661–3666 (2013).
16. Haigh, I. D. *et al.* Timescales for detecting a significant acceleration in sea level rise. *Nature Commun.* **5,** 3635 (2014).
17. Taylor, K. E., Stouffer, R. J. & Meehl, G. A. An overview of CMIP5 and the experiment design. *Bull. Am. Meteorol. Soc.* **93,** 485–498 (2012).
18. Slangen, A. B. A. *et al.* Projecting twenty-first century regional sea-level changes. *Climatic Change* **124,** 317–332 (2014).
19. Church, J. A. *et al.* Revisiting the Earth's sea-level and energy budgets from 1961 to 2008. *Geophys. Res. Lett.* **38,** L18601 (2011).
20. Mitrovica, J. X. *et al.* On the robustness of predictions of sea level fingerprints. *Geophys. J. Int.* **187,** 729–742 (2011).
21. Van Vuuren, D. P. *et al.* The representative concentration pathways: An overview. *Climatic Change* **109,** 5–31 (2011).
22. Hawkins, E. *et al.* Uncertainties in the timing of unprecedented climates. *Nature* **511,** E3–E4 (2014).
23. Yin, J. & Goddard, P. B. Oceanic control of sea level rise patterns along the East Coast of the United States. *Geophys. Res. Lett.* **40,** 5514–5520 (2013).
24. Meehl, G. A. *et al.* Relative outcomes of climate change mitigation related to global temperature versus sea-level rise. *Nature Clim. Change* **2,** 576–580 (2012).
25. Bouttes, N., Gregory, J. M. & Lowe, J. A. The reversibility of sea level rise. *J. Clim.* **26,** 2502–2513 (2013).
26. Sutton, R. T., Dong, B. & Gregory, J. M. Land/sea warming ratio in response to climate change: IPCC AR4 model results and comparison with observations. *Geophys. Res. Lett.* **34,** L02701 (2007).
27. Slangen, A. B. A., van de Wal, R. S. W., Wada, Y. & Vermeersen, L. L. A. Comparing tide gauge observations to regional patterns of sea-level change (1961–2003). *Earth Syst. Dynam.* **5,** 243–255 (2014).
28. Sen Gupta, A., Jourdain, N. C., Brown, J. N. & Monselesan, D. Climate drift in the CMIP5 models. *J. Clim.* **26,** 8597–8615 (2013).
29. Schotman, H. H. A. & Vermeersen, L. L. A. Sensitivity of glacial isostatic adjustment models with shallow low-viscosity earth layers to the ice-load history in relation to the performance of GOCE and GRACE. *Earth Planet. Sci. Lett.* **236,** 828–844 (2005).
30. Kendall, R. A., Mitrovica, J. X. & Milne, G. A. On post-glacial sea level–II. Numerical formulation and comparative results on spherically symmetric models. *Geophys. J. Int.* **161,** 679–706 (2005).

Acknowledgements

We acknowledge the World Climate Research Programme's Working Group on Coupled Modelling, which is responsible for CMIP, and we thank the climate modelling groups for producing and making available their model output. For CMIP, the US Department of Energy's Program for Climate Model Diagnosis and Intercomparison provides coordinating support and leads development of software infrastructure in partnership with the Global Organization for Earth System Science Portals. We thank AVISO (http://www.aviso.oceanobs.com) for providing altimeter data. We also thank D. Monselesan for help with CMIP5 data handling. Detailed comments on an early draft by M. King and J. Hunter helped to improve the manuscript significantly. J.A.C. and X.Z. are supported by the Australian Climate Change Science Program (ACCSP). K.L. and J.H. are supported by the China Scholarship Council and the National Natural Science Foundation of China (41276006). A.B.A.S. is funded by a CSIRO Office of the Chief Executive Postdoctoral Fellowship.

Author contributions

X.Z. conceived and designed the study with K.L. K.L. carried out the analysis and produced all figures under the guidance of X.Z. and J.A.C. A.B.A.S. prepared the regional sea-level projection data for land ice and groundwater contributions. K.L. wrote the first draft with X.Z., and all authors made contributions to writing the manuscript.

Additional information

Supplementary information is available in the online version of the paper. Reprints and permissions information is available online at www.nature.com/reprints. Correspondence and requests for materials should be addressed to X.Z.

Competing financial interests

The authors declare no competing financial interests.

The author has requested enhancement of the downloaded file. All in-text references underlined in blue are linked to publications on ResearchGate.

© 2014 Macmillan Publishers Limited. All rights reserved.